ISSN 0015-4628, Fluid Dynamics, 2017, Vol. 52, No. 4, pp. 547–560. © Pleiades Publishing, Ltd., 2017.
Original Russian Text © M.M. Alimov, K.G. Kornev, 2017, published in Izvestiya Rossiiskoi Akademii Nauk, Mekhanika Zhidkosti i Gaza, 2017, No. 4, pp. 97–112.

An External Meniscus on a Thin Ovoidal Fiber (The Case of Full Wetting)

M. M. Alimov[a*] **and K. G. Kornev**[b]

[a] *Kazan Federal University, ul. Kremlevskaya 18, Kazan, 420008 Russia*
[b] *Clemson University, Clemson, SC, USA*
e-mail: [*] *Mars.Alimov@kpfu.ru*

Received November 14, 2016

Abstract—A complex shape of an external meniscus formed due to the capillary rise of a liquid along a fiber having the ovoidal profile is considered. Within the framework of the asymptotic approach and under the assumption on the complete wetting of the fiber material by the liquid, an analytical solution of the problem is derived. The particular examples of the meniscus configuration are presented in the cases in which the fiber profile has the shape of an ovoid or an ellipse.

Keywords: capillary rise, minimum surfaces, matching of asymptotic expansions.

DOI: 10.1134/S0015462817040093

When an isolated fiber is immersed into a liquid, the capillary rise of the liquid along the fiber changes the shape of the free surface of the liquid and forms, as a result, an external meniscus. The meniscus configuration is determined by both the fiber profile and the wetting properties of the fiber surface [1–3]. The menisci formed by round fibers are fairly well studied [4–8]. There are also some studies [6, 9–11], in which the numerical and asymptotic methods were applied to investigate the menisci formed by fibers with a smooth, near-circular profile.

In particular, in [11] shape of the meniscus on a fiber of elliptical cross-section was determined using numerical methods. An analysis of the results of that study revealed an important limitation of the computational difference methods: they lose their effectiveness in the case of small contact angles characterizing the wettability of the fiber material. This is attributable to the fact that in the case of small contact angles the level function describing the meniscus shape is characterized by large, and in the case of complete wetting even infinite, gradient values on the fiber surface. This seems an almost undefeatable obstacle in direct numerical simulation of the problem using the difference methods. Thus, in the above-mentioned study [11] the smallest calculated value of the contact angle was about $\pi/3$.

In [12] an asymptotic approach to an analysis of the configuration of an external meniscus on a fiber with an arbitrary profile was developed under the condition of the smallness of its characteristic dimension compared to the capillary length. Below it is shown that in the case of complete wetting the methods developed in [12] can be applied to the derivation of an analytical solution of the problem of the meniscus shape for the fibers, whose profiles belong to a certain class of smooth convex profiles.

1. FORMULATION OF THE PROBLEM

Let as a result of fiber immersion into a liquid there be formed an external meniscus Σ with the contact line Γ_c on the interface of three media, namely, the air, the liquid, and the fiber material (Fig. 1a). The profile of the normal section Γ of the fiber is smooth, convex, and has one axis of symmetry (it is the x axis in Fig. 1b).

We will take half profile thickness along the axis of symmetry for the scale length L_m: $L_m = |BD|/2$. Apart from this length, one more scale can be introduced in the problem; this is the capillary length

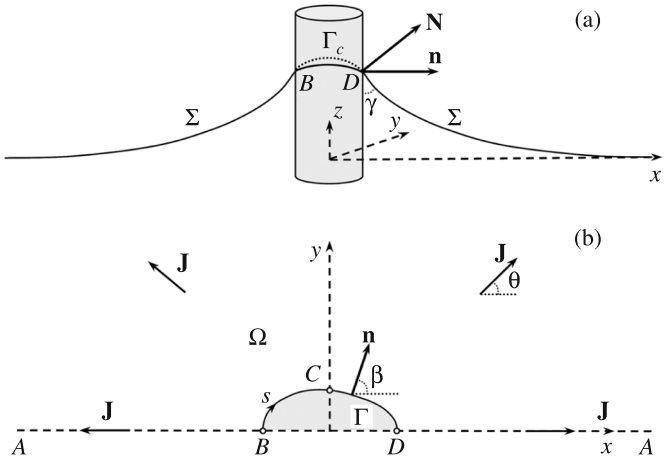

Fig. 1. View of a meniscus in space (a) and upper half of the physical plane $x,\ y$ (b).

$L_c = \sqrt{\sigma_s/(\rho g)}$, where σ_s is the surface tension, ρ is the liquid density, and g is the gravity acceleration. Correspondingly, the capillary rise under consideration is characterized by the dimensionless complex, or the Bond number ε [13]

$$\varepsilon = \frac{L_m^2}{L_c^2} = \frac{\rho g}{\sigma_s} L_m^2.$$

Basing on the scale length L_m we will introduce the dimensionless Cartesian coordinate system $x,\ y,\ z$ such that the z axis is the central axis of the fiber, the x axis is orthogonal to the fiber axis and aligned with the axis of symmetry of the profile, and the $(x,\ y)$ plane is tangent to the meniscus surface at infinity, as $r \to \infty$, where $r = \sqrt{x^2 + y^2}$. The meniscus surface Σ is given by the function

$$z = h(x,\ y),$$

where h is the dimensionless height of the liquid column at the point $(x,\ y)$ measured from the liquid level at infinity.

Since the fiber profile possesses the symmetry about the x axis, the same symmetry is inherent in the meniscus surface Σ and the function $h(x,\ y)$. For this reason, it is possible to introduce a symmetry element of the physical $(x,\ y)$ plane, namely, the domain $\Omega = ABDA$, which represents the upper half of the outside of the normal section of the fiber (Fig. 1b). Then the mathematical model of the capillary rise of a liquid along this fiber can be written in the form of the boundary value problem for the function $h(x,\ y)$ in domain Ω [6]

$$\Omega: \quad \nabla \cdot \left[(1 + |\nabla h|^2)^{-1/2} \nabla h\right] - \varepsilon h = 0, \tag{1.1}$$

$$A: \quad h|_{r\to\infty} \to 0, \tag{1.2}$$

$$AB \cup DA: \quad \frac{\partial h}{\partial y} = 0, \tag{1.3}$$

$$\Gamma = BD: \quad (1 + |\nabla h|^2)^{-1/2} \nabla h \cdot \mathbf{n} = -\cos\gamma, \tag{1.4}$$

where $\Gamma \equiv BD$ is the boundary of the fiber profile in the upper half-plane $x,\ y$ and, at the same time, the projection of the contact line Γ_c on the plane $x,\ y$; γ is the contact angle characterizing the liquid-air-fiber material triad, and $\mathbf{n}$ is the outward normal to fiber profile boundary Γ, which can be formalized by means of introducing the angle of inclination β of the normal $\mathbf{n}$ to the x axis (see Fig. 1b)

$$\mathbf{n} = (\cos\beta,\ \sin\beta). \tag{1.5}$$

On the intervals AB and DA the conditions of smooth symmetric continuation are fulfilled, while the Young–Laplace condition of the dynamic equilibrium of the contact line Γ_c is imposed on boundary Γ (Fig. 1a).

We note that the contact angle varies within the limits $\gamma \in [0,\ \pi/2)$, when the fiber material is wetted by the liquid, and, otherwise. within the limits $\gamma \in (\pi/2,\ \pi]$. Since in the cases in which $\gamma = \gamma^0$ and $\gamma = \pi - \gamma^0$ the solutions of problem (1.1)–(1.5) differ only in the sign ahead of $h(x,\ y)$, it is sufficient to consider the wetting case $\gamma \in [0,\ \pi/2)$.The case $\gamma = \pi/2$ is not considered, since it is associated with the trivial solution $h \equiv 0$.

If the fiber is thin, $L_a \ll L_c$, then the Bond number is small, $\varepsilon \ll 1$, and asymptotic methods, in particular, the method of matching asymptotic expansions [12], can be employed. The inner asymptotic expansion $h^{(i)}(x,\ y)$ of the function $h(x,\ y)$ in ε is valid in the vicinity of the fiber, while the outer expansion is valid in the vicinity of infinity, when $r \to \infty$. For any fiber profile the principal term of the outer expansion $h^{(o)}(x,\ y)$ takes the form:

$$h^{(o)}(x,\ y) = \frac{l\cos\gamma}{2\pi} K_0(r\sqrt{\varepsilon}), \tag{1.6}$$

where l is the dimensionless perimeter of the fiber profile, that is, the doubled perimeter of the profile Γ, and K_0 is the Bessel function of the second kind. For the principal term of the inner asymptotic expansion $h^{(i)}(x,\ y)$ the following boundary value problem can be formulated [12]

$$\Omega: \quad \nabla \cdot \left[(1 + |\nabla h^{(i)}|^2)^{-1/2} \nabla h^{(i)}\right] = 0, \tag{1.7}$$

$$A: \quad h^{(i)} = -l\cos\gamma (2\pi)^{-1} \ln(e^E \sqrt{\varepsilon} r/2) + O(r^{-1})|_{r\to\infty}, \tag{1.8}$$

$$AB \cup DA: \quad \frac{\partial h^{(i)}}{\partial y} = 0, \tag{1.9}$$

$$\Gamma \equiv BD: \quad (1 + |\nabla h^{(i)}|^2)^{-1/2} \nabla h^{(i)} \cdot \mathbf{n} = -\cos\gamma, \tag{1.10}$$

where $E = 0.57\ldots$ is the Euler constant.

In the principal term of the inner asymptotic expansion the differential equation (1.7) does not include the term with the hydrostatic pressure, while the condition at infinity is the result of the matching with the principal term of the outer expansion (1.6) [12]. Taking account for the first-order term on the right side of the condition at infinity (1.8) is necessary, since in the original problem (1.1)–(1.5) the height $h(x,\ y)$ is measured from the liquid level at infinity, as $r \to \infty$, while the infinity is not encompassed by the inner expansion (1.5),(1.7)–(1.10). Thus, the inner expansion has none of the characteristic points of the plane $(x_*,\ y_*)$ with a known absolute value $h(x_*,\ y_*)$ from which the function $h^{(i)}(x,\ y)$ could be measured. Correspondingly, in solving the boundary value problem (1.5),(1.7)–(1.10), that is, in essence, in integrating a partial differential equation, the problem of determining the integration constant arises. Only taking account for the first-order term in the boundary condition (1.8) gives a hope for the effective solution of this problem.

If, as a result, of the solution of problem (1.5), (1.7)–(1.10), the principal term of the inner expansion $h^{(i)}(x,\ y)$ has been determined, the principal term $h^{(u)}(x,\ y)$ of the asymptotic expansion of $h(x,\ y)$ in ε, uniformly approximating the solution $h(x,\ y)$ of problem (1.1)–(1.5) throughout the entire plane $x,\ y$ can be determined according to the Van Dyke formula [14]

$$h^{(u)}(x,\ y) = h^{(i)}(x,\ y) + \frac{l\cos\gamma}{2\pi}\left\{K_0(r\sqrt{\varepsilon}) + \ln\left[\frac{r\sqrt{\varepsilon}\exp(E)}{2}\right]\right\}. \tag{1.11}$$

It remains to determine the solution of the boundary value problem for the inner expansion (1.5), (1.7)–(1.10).

2. ANALOGY WITH FILTRATION OF ANOMALOUSLY VISCOUS FLUIDS. CHAPLYGIN TRANSFORMATION

Although Eq. (1.7) is the equation of a minimum surface, the boundary value problem (1.5), (1.7)–(1.10) considerably differs from the problems of theory of minimum surfaces [15] in its specific boundary conditions (1.8) and (1.10). At the same time, in [12] it was established that in an analysis of this problem the analogy with the problems of seepage flow of anomalously viscous fluids in a porous medium [16] can effectively be used. We will define the fictitious hydrodynamic flux $\mathbf{J}$ of the fluid as follows:

$$\mathbf{J} = -\frac{\nabla h^{(i)}}{|\nabla h^{(i)}|} J, \qquad J = \frac{|\nabla h^{(i)}|}{\sqrt{1 + |\nabla h^{(i)}|^2}}, \tag{2.1}$$

where the root is arithmetic. The flux vector $\mathbf{J}$ is characterized by its value $J = |\mathbf{J}|$ and the angle of inclination to the x axis θ.

The relationship between the quantities J and $|\nabla h^{(i)}|$ can also be written in another form:

$$|\nabla h^{(i)}| = \Phi(J), \qquad \Phi(J) = \frac{J}{\sqrt{1-J^2}}, \tag{2.2}$$

where $\Phi(J) \geq 0$ and $\Phi'(J) \geq 0$. Correspondingly, the differential equation (1.7) can be represented in the form of a system of differential equations governing the fictitious seepage flow of an anomalous fluid in a porous medium [16]

$$\Omega: \quad \nabla h^{(i)} = -\frac{\mathbf{J}}{J}\Phi(J), \qquad \nabla \cdot \mathbf{J} = 0. \tag{2.3}$$

In this case $h^{(i)}(x,\ y)$ is the counterpart of the head and $\mathbf{J}(x,\ y)$ is the counterpart of the seepage flow velocity. The flow behavior is presented in Fig. 1b for the case in which $\gamma < \pi/2$. In particular, certain examples of the seepage flows obeying law (2.2) had been considered by V.V. Sokolovskii [17].

The second differential equation (2.3) means that the fluid is incompressible and, therefore, the stream function $\psi(x,\ y)$ can be introduced [18]. Then we have

$$J_x = J\cos\theta = \frac{\partial\psi}{\partial y}, \qquad J_y = J\sin\theta = -\frac{\partial\psi}{\partial x}, \tag{2.4}$$

while the system of differential equations (2.3) can be written in the form:

$$\frac{\partial h^{(i)}}{\partial x} = -\Phi(J)\cos\theta, \quad \frac{\partial h^{(i)}}{\partial y} = -\Phi(J)\sin\theta, \quad \frac{\partial\psi}{\partial x} = -J\sin\theta, \quad \frac{\partial\psi}{\partial y} = J\cos\theta. \tag{2.5}$$

As shown by Khristianovich [17, 19], in studying the seepage flows obeying law (2.3) it is convenient to use the Chaplygin transformation [20] to the velocity hodograph variables $t,\ \theta$, where t and J are related by the expression

$$J = \frac{1}{\cosh t}, \qquad t = \operatorname{arccosh}\frac{1}{J}, \qquad \Phi(J) = \frac{1}{\sinh t}. \tag{2.6}$$

In fact, let us transform the system of equations (2.5) to the variables $J,\ \theta$

$$\frac{\Phi^2(J)}{J\Phi'(J)}\frac{\partial\psi}{\partial J} = -\frac{\partial h^{(i)}}{\partial\theta}, \qquad \frac{\Phi(J)}{J^2}\frac{\partial\psi}{\partial\theta} = \frac{\partial h^{(i)}}{\partial J}.$$

Substituting the particular form (2.2) of the function $\Phi(J)$ into this equation, passing from the variable J to the variable t, and taking expressions (2.6) into account we arrive at the Cauchy–Riemann relations

$$\frac{\partial\psi}{\partial t} = \frac{\partial h^{(i)}}{\partial\theta}, \qquad \frac{\partial\psi}{\partial\theta} = -\frac{\partial h^{(i)}}{\partial t}.$$

Therefore, we can introduce the complex variables W and χ [21]

$$W = -h^{(i)} + i\psi, \qquad \chi = t + i\theta \tag{2.7}$$

and use the functions of a complex variable $W(\chi)$ and $\chi(W)$. Conditionally, W is called the complex potential of the flow and χ is the velocity hodograph [16].

If, say, the function $\chi(W)$ would be determined, we can return into the physical plane $x,\ y$ writing down the Khristianovich formulas of the full differentials of the functions $x(h^{(i)},\ \psi)$ and $y(h^{(i)},\ \psi)$ [16, 19]

$$dx = -\cos\theta\sinh t\, dh^{(i)} - \sin\theta\cosh t\, d\psi, \quad dy = -\sin\theta\sinh t\, dh^{(i)} + \cos\theta\cosh t\, d\psi. \tag{2.8}$$

We note that, in its meaning, the quantity $|\nabla h^{(i)}|$ can generally vary in the physical plane from 0 to ∞. In view of relations (2.2) between $|\nabla h^{(i)}|$ and J and (2.6) between J and t, it can easily be seen that, as $|\nabla h^{(i)}| \to 0$, $J \to 0$ and $t \to \infty$ and, as $|\nabla h^{(i)}| \to \infty$, $J \to 1$ and $t \to 0$. Therefore, everywhere in the closure $[\Omega]$ of the domain Ω, including the boundary Γ and infinity, there hold the restrictions on the quantities J and t

$$[\Omega]: \quad 0 < J \leq 1, \qquad 0 \leq t < \infty. \tag{2.9}$$

3. COMPLEX PLANE

We will express the boundary conditions of problem (1.5), (1.7)–(1.10) in terms of the complex variables W and χ. From the considerations of flow symmetry it follows that the rays BA and DA are streamlines, on any of which ψ is constant (see Fig. 1b). These constants can be determined by estimating the flow behavior at infinity. From the boundary condition (1.8) at infinity there follows the estimate

$$A: \quad \nabla h^{(i)} = -\frac{l\cos\gamma}{2\pi r^2}\mathbf{r} + O(r^{-2})|_{r\to\infty}. \tag{3.1}$$

Substituting this estimate into expression (2.1) we obtain the estimate for the flux $\mathbf{J}$ in the vicinity of infinity: $\mathbf{J} \approx -\nabla h^{(i)}$. In view of flow incompressibility, this means that in the vicinity of infinity there is a potential sink flow of the intensity $l\cos\gamma$ [18]. Then the boundary conditions of problem (1.9) on the intervals AB and DA can be written in terms of the variables W and χ as follows:

$$DA: \quad \psi = 0, \quad \theta = 0; \qquad AB: \quad \psi = 0.5l\cos\gamma, \quad \theta = \pi. \tag{3.2}$$

Preliminarily, we will express the boundary condition (1.10) on Γ in terms of the flux $\mathbf{J}$

$$\Gamma: \quad \mathbf{J}\cdot\mathbf{n} = \cos\gamma, \tag{3.3}$$

whereupon, using expression (1.5) of the normal $\mathbf{n}$ in terms of the angle β and relation (2.6) between the quantities J and t, we obtain the required form of condition (1.10) in terms of the velocity hodograph variables t and θ

$$\Gamma: \quad \cos(\theta - \beta) = \cos\gamma\cosh t. \tag{3.4}$$

Finally, rewriting the condition at infinity (1.8) in terms of Eqs. (2.1) and (2.6) yields

$$A: \quad -h^{(i)}(x, y)|_{r\to\infty} \sim \frac{l\cos\gamma}{2\pi}\ln r \to \infty, \qquad J \to 0, \qquad t \to \infty. \tag{3.5}$$

Thus, problem (1.5), (1.7)–(1.10) is reduced to problem (3.2), (3.4), (3.5) of determining an analytical function of the complex variable $\chi(W)$ followed by the reconstruction of two real functions $x(h^{(i)}, \psi)$ and $y(h^{(i)}, \psi)$ using the Khristianovich relations (2.8).

As in theory of ideal fluid jets [22], we will use the flow parametrization which is understood to mean the introduction of an auxiliary plane of the parametric complex variable $\zeta = \xi + i\eta$ of the canonical form and the reduction of the problem of determining three functions $\chi(W)$, $x(h^{(i)}, \psi)$, and $y(h^{(i)}, \psi)$ to the problem of determining four functions, namely, two functions $W = W(\zeta)$ and $\chi = \chi(\zeta)$ of the complex variable ζ and two real functions $x = x(\xi, \eta)$ and $y = y(\xi, \eta)$. As the auxiliary plane $\zeta = \xi + i\eta$ we will take the plane in which the fictitious flow domain Ω corresponds to the upper half of the unit circle Ω_ζ (Fig. 2a).

The presence of the complex variables (2.7) indicates that, possibly, the problem solution can be effectively constructed using the velocity hodograph method [22]. In particular, in theory of seepage flow of anomalous fluids [16] this method was applied to construct a lot of nontrivial solutions, which are exact in the sense of determining the closed form of the functions $W(\zeta)$ and $\chi(\zeta)$. However, the necessary condition of the effectiveness of the velocity hodograph method is the known canonical form of the planes W and χ.

The formulation of the problem (3.2), (3.4), and (3.5) written above differs from the formulation of the seepage flow problem [16] in the specific condition on the fiber boundary (3.4). It contains none of the parts of the variable W, while the two parts of the variable χ are related by the angle of inclination of the normal β, whose relation with the angle $\sigma = \arg(\zeta)$ should be established. All this does not show promise of directly determining the form of the planes χ and W and, therefore, effectively using the velocity hodograph method in the general case of the wetting $\gamma \in [0, \pi/2)$. For this reason, in what follows we will restrict ourselves to the simplest case of complete wetting $\gamma = 0$.

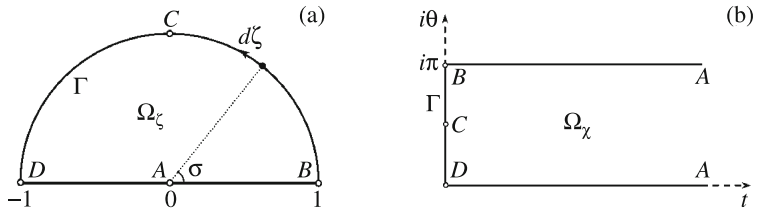

Fig. 2. Views of the auxiliary plane ζ (a) and the velocity hodograph plane χ (b).

4. DETERMINATION OF THE FUNCTIONS $\chi(\zeta)$ AND $W(\zeta)$ IN THE CASE OF THE COMPLETE WETTING $\gamma = 0$

Owing to the general restriction $J \le 1$ (Eq. (2.9)) in the $\gamma = 0$ case condition (3.3) on the boundary Γ can be satisfied then and only then, when the flux vector **J** is directed along the normal **n** to the boundary Γ and its value is unity [12]. Then, in view of Eq. (2.6), everywhere on Γ we obtain

$$\Gamma: \quad \theta = \beta, \qquad J = 1, \qquad t = 0. \tag{4.1}$$

In view of the boundary conditions (3.2) and (3.5), we can convince ourselves that the flow domain Ω in the physical plane is associated with the half-band Ω_χ in the hodograph plane χ (Fig. 2b). Obviously, this fact is valid for any smooth and convex fiber profile, when β monotonically changes along the profile. As a result, we obtain the canonical form of the hodograph plane χ and the function $\chi(\zeta)$ can be found using the method of conformal mappings [12]

$$\chi(\zeta) = \ln[\zeta^{-1}\exp(i\pi)], \quad t = -\ln|\zeta|, \quad \theta = \pi - \arg\zeta. \tag{4.2}$$

In particular, Eqs. (4.1) and (4.2) make it possible to determine the direct relation between the angle β and θ and σ

$$\Gamma: \quad \theta \equiv \beta = \pi - \sigma. \tag{4.3}$$

We will now turn to the determination of the function $W(\zeta)$. In view of relation (2.4) between the flux vector **J** and the stream function ψ and the fact that on Γ the quantity $J = 1$, we can write the differential boundary relation

$$\Gamma: \quad d\psi_\Gamma/d\sigma = -ds/d\sigma < 0, \tag{4.4}$$

where s is the arclength of the profile Γ measured from point B.

Since the fiber profile shape is known, the dependence of the angle β of inclination of the normal to the profile on the arc abscissa s, that is, the function $\beta(s)$, can be established, together with the derivatives $\beta'(s)$ and $s'(\beta)$. We will denote the latter function by $F(\beta)$

$$\Gamma: \quad F(\beta) = -ds/d\beta > 0. \tag{4.5}$$

Obviously that it has the meaning of the radius of curvature of the profile Γ as a function of the angle β of the inclination of the normal to the profile.

Since the angles β and σ are related by the simple equation (4.3), the right side of Eq. (4.4) can be expressed in terms of function $F(\beta)$

$$\sigma \in [0,\ 2\pi], \qquad ds/d\sigma = F(\beta)|_{\beta=\pi-\sigma} \equiv F_*(\sigma) > 0. \tag{4.6}$$

Equations (4.4) and (4.6) mean that the derivative $d\psi/d\sigma$ is known on the profile Γ, which makes it possible to reconstruct first the derivative $dW/d\zeta$ and then the function $W(\zeta)$ itself. In fact, let us introduce the auxiliary function $\omega(\zeta)$ of the form:

$$\omega(\zeta) = \zeta(dW/d\zeta). \tag{4.7}$$

The following boundary relation is always fulfilled on the profile Γ in the ζ plane

$$\Gamma: \quad \omega(\zeta)|_{\zeta=\exp(i\sigma)} = -i\frac{d}{d\sigma}\left(-h_\Gamma^{(i)} + i\psi_\Gamma\right) = \frac{d\psi_\Gamma}{d\sigma} + i\frac{dh_\Gamma^{(i)}}{d\sigma},$$

whence it follows that on the profile Γ $d\psi_\Gamma/d\sigma = \mathrm{Re}\,\omega(\zeta)$. Finally, rewriting Eq. (4.4) in terms of Eq. (4.6) yields the boundary condition for the function $\omega(\zeta)$

$$\Gamma: \quad \mathrm{Re}\,\omega(\zeta)|_{\zeta=\exp(i\sigma)} = -F_*(\sigma). \tag{4.8}$$

If the function $\omega(\zeta)$ is regular in the unit circle $|\zeta| \le 1$, then Eq. (4.8) represents the well-known Schwarz problem [23]. The regularity of $\omega(\zeta)$ is in doubt because of point $A: \ \zeta = 0$, since it was found that both functions $h^{(i)}(r)$ and $\chi(\zeta)$ have the logarithmic singularities at this point (cf. Eqs. (3.5) and (4.2), respectively). To elucidate this question it is sufficient to analyze the behavior of the function $W(\zeta)$ at the point $A: \ \zeta = 0$.

In accordance with the boundary conditions (3.2), the harmonic function $\psi(\xi, \ \eta)$ experiences a jump at point A. This means that the conjugate function $h^{(i)}(\xi, \ \eta)$ has the logarithmic singularity at this point [21]. Its particular form can be found using the boundary condition (1.8) at point A but for this purpose the behavior of the function $x(\xi, \ \eta)$ must be formalized, as $x \to \infty$.

In the vicinity of infinity of the physical plane the quantity $|\nabla h^{(i)}|$ is small (see estimate (3.1)) and here the differential equation (1.7) transforms into the Laplace equation. For this reason, similarly to the case of the Laplace equation, the behavior of the function $x(\xi, \ \eta)$ in the vicinity of point A can be formally preassigned using an indefinite constant $A_\infty > 0$ [21]

$$\eta = 0, \qquad |\xi| \ll 1: \quad x = -A_\infty \xi^{-1} \ + \ O(1). \tag{4.9}$$

The vicinity $\eta = 0$, $|\xi| \ll 1$ of point A in the ζ plane is associated with the vicinity $y = 0$, $r = |x| \sim \infty$ of point A in the physical plane. Then from the boundary condition at infinity (1.8) for $\gamma = 0$ and Eq. (4.9) there follows the estimate

$$\eta = 0, \quad |\xi| \ll 1: \quad h^{(i)}(\xi, \ \eta) = \frac{1}{2\pi} \ln\left[\frac{2|\xi|}{A_\infty \sqrt{\varepsilon}\exp(E)}\right] \ + \ O(\xi). \tag{4.10}$$

Using this estimate, together with the boundary conditions (3.2), we can exactly separate out the form of the main part of the function $W(\zeta)$ containing the logarithmic singularity

$$W(\zeta) = \frac{l}{2\pi} \ln\left[\zeta^{-1}\exp(i\pi)\right] \ + \ W_r(\zeta). \tag{4.11}$$

The boundary conditions for the regular part $W_r(\zeta)$ of the function $W(\zeta)$ are homogeneous on the intervals AB and DA: $AB \cup DA$, $\mathrm{Im}\, W_r = 0$. Therefore, the function $W_r(\zeta)$ can be symmetrically continued to the lower half of the unit circle $|\zeta| \le 1$ and can be represented there in the form of a series with real coefficients w_k

$$W_r(\xi, \ \eta) = w_0 \ + \ \sum_{k=1}^{\infty} w_k \zeta^k. \tag{4.12}$$

From expressions (4.11) and (4.12) it follows directly that the function $\omega(\zeta)$ of form (4.7) is regular everywhere within the unit circle $|\zeta| \le 1$ and can be represented in the series form

$$\omega(\zeta) = -\frac{l}{2\pi} \ + \ \sum_{k=1}^{\infty} k w_k \zeta^k. \tag{4.13}$$

Thus, expression (4.8) really represents the Schwarz problem for the function $\omega(\zeta)$ regular in the unit circle $|\zeta| \le 1$. As is known [23], its solution can be written in the form of the Schwarz integral

$$\omega(\zeta) = -\frac{1}{2\pi} \int_0^{2\pi} F_*(\sigma) \frac{\exp(i\sigma) \ + \ \zeta}{\exp(i\sigma) \ - \ \zeta} d\sigma \ + \ iC. \tag{4.14}$$

where $F_*(\sigma)$ has the form (4.6) and C is the real integration constant. To determine this constant we will use the fact that at point $\zeta = 0$ the value of the function $\omega(\zeta)$ is completely determined: $\omega(0) = -l/(2\pi)$ (see Eq. (4.13)). Then from Eq. (4.14) we can determine the value of C and derive the expression for the fiber perimeter l

$$C = 0, \quad l = 2\int_0^\pi F_*(\sigma)\, d\sigma.$$

Thus, the function $\omega(\zeta)$ is completely determined, the coefficients of its representation (4.13) are known, and the coefficients w_k of representation (4.12) of the function $W_r(\zeta)$ can be reconstructed accurate to the indefinite real integration constant w_0.

5. RECONSTRUCTION OF THE FUNCTION $h^{(i)}(x, y)$

Using expressions (2.7) and (4.11) we will write the function $h^{(i)}(\xi, \eta)$ in the form:

$$h^{(i)}(\xi, \eta) = \frac{l}{2\pi}\ln|\zeta| - \mathrm{Re}\, W_r(\zeta).$$

Hence, with account for expression (4.12), there follows the estimate for the function $h^{(i)}(\xi, \eta)$ in the vicinity of point A belonging to the boundary $AB \cup DA$ in the ζ plane

$$\eta = 0, \quad |\xi| \ll 1: \quad h^{(i)}(\xi, 0) = \frac{l}{2\pi}\ln|\xi| - w_0 + O(\xi).$$

Comparing this estimate with the earlier derived estimate (4.10) we can find the relation between the integration constant w_0 and the earlier formally-introduced parameter A determining the behavior (4.9) of the function $x(\xi, \eta)$ in the vicinity of point A

$$w_0 = \frac{l}{2\pi}\ln\left[\frac{A_\infty\sqrt{\varepsilon}\exp(E)}{2}\right]. \tag{5.1}$$

To determine the parameter A_∞ we will use the estimate of the behavior of the function $t(\xi, \eta)$ in the vicinity $\eta = 0$, $|\xi| \ll 1$ of point A. On one hand, having the exact form (4.2) of the function $\chi(\zeta)$ we can give the accurate estimate

$$\eta = 0, \quad |\xi| \ll 1: \quad t(\xi, \eta) = -\ln|\xi|. \tag{5.2}$$

On the other hand, an approximate estimate of the behavior of the function $t(\xi, \eta)$ in the vicinity $\eta = 0$, $|\xi| \ll 1$ of point A in the ζ plane can be derived on the basis of the boundary condition (1.8). To do this, some auxiliary estimates must be made.

We will first substitute condition (3.1) at $\gamma = 0$ into Eq. (2.1) and obtain the estimate of the quantity J in the vicinity $r = |x| \sim \infty$ of point A in the physical plane

$$r = |x| \sim \infty: \quad J = \frac{l}{2\pi|x|}\left[1 + O(|x|^{-1})\right].$$

In view of relation (2.6) between J and t, we can write this estimate in the form:

$$r = |x| \sim \infty: \quad t = \mathrm{arccosh}\,[2\pi l^{-1}|x| + O(1)].$$

Using Eq. (4.9) we pass to the vicinity $\eta = 0$, $|\xi| \ll 1$ of point A in the ζ plane

$$\eta = 0, \quad |\xi| \ll 1: \quad t = \mathrm{arccosh}\,[2\pi A_\infty l^{-1}|\xi|^{-1} + O(1)].$$

Writing the function arccosh of a large argument we obtain an approximate estimate of the behavior of the function $t(\xi, \eta)$ in the vicinity $\eta = 0$, $|\xi| \ll 1$

$$\eta = 0, \quad |\xi| \ll 1: \quad t(\xi, \eta) = -\ln|\xi| + \ln(4\pi A_\infty l^{-1}) + O(|\xi|). \tag{5.3}$$

Let us compare estimates (5.2) and (5.3). They agree with one another only provided that $A_\infty = l/(4\pi)$. Substituting the parameter A_∞ thus obtained into Eq. (5.1) we definitively determine the value of the integration constant w_0

$$w_0 = \frac{l}{2\pi}\ln\left[\frac{l\sqrt{\varepsilon}\exp(E)}{8\pi}\right].$$

As a result, all the coefficients of series (4.12) representing the function $W(\zeta)$ are found. Moreover, the form of the function $W(\zeta)$ can be analytically reconstructed taking account for definition (4.7) of the function $\omega(\zeta)$ and Eq. (4.11)

$$W(\zeta) = \frac{l}{2\pi}\ln\left[\zeta^{-1}\exp(i\pi)\right] + w_0 + \int_0^\zeta \left[\omega(\zeta) + \frac{l}{2\pi}\right]\frac{d\zeta}{\zeta}.$$

Separating out the real part of $W(\zeta)$ we can determine the function $h^{(i)}(\xi, \eta)$ everywhere in domain Ω_ζ and, in particular, the dependence $h_\Gamma^{(i)}(\sigma)$ on the boundary $\Gamma:\ \zeta = \exp(i\sigma)$.

Then, in order to reconstruct the dependences $x_\Gamma(\sigma)$ and $y_\Gamma(\sigma)$ on the boundary $\Gamma:\ \zeta = \exp(i\sigma)$ in the auxiliary plane we will write down the Khristianovich relations (2.8) in terms of expressions (4.3), (4.4), amd (4.6)

$$\Gamma:\ \frac{dx_\Gamma}{d\sigma} = -\sin\theta_\Gamma(\sigma)\frac{d\psi_\Gamma}{d\sigma} = \sin\sigma F_*(\sigma), \qquad \frac{dy_\Gamma}{d\sigma} = \cos\theta_\Gamma(\sigma)\frac{d\psi_\Gamma}{d\sigma} = \cos\sigma F_*(\sigma)$$

and integrate them. The form of the dependences $x_\Gamma(\sigma)$, $y_\Gamma(\sigma)$, and $h_\Gamma^{(i)}(\sigma)$ thus obtained makes it possible to reconstruct the distribution of $h_\Gamma^{(i)}(x, y)$ on the boundary Γ in the physical plane.

Finally, we can determine the distribution of $h^{(i)}(x, y)$ throughout the entire flow domain in the physical plane. In fact, the function $h^{(i)}(\xi, \eta)$ is known, while the functions $x(\xi, \eta)$ and $y(\xi, \eta)$ can be reconstructed using the Khristianovich relations (2.8) in the form:

$$\begin{aligned} dx &= -\cos\theta\sinh t\, dh^{(i)}(\xi, \eta) - \sin\theta\cosh t\, d\psi(\xi, \eta), \\ dy &= -\sin\theta\sinh t\, dh^{(i)}(\xi, \eta) + \cos\theta\cosh t\, d\psi(\xi, \eta) \end{aligned} \tag{5.4}$$

and integrating them on a radial grid in the ζ plane starting from the points on the boundary $\Gamma:\ \zeta = \exp(i\sigma)$. Thus, we determine the configuration of the meniscus $\Sigma^{(i)}$ corresponding to the inner asymptotic expansion of problem (1.1)–(1.5). Thereupon, the distribution of $h^{(u)}(x, y)$ can be found using Eq. (1.11).

Thus, the asymptotic expansion uniformly approximating the solution $h(x, y)$ of problem (1.1)–(1.5) is analytically obtained throughout the entire physical plane for a smooth convex fiber profile with the known function $F(\beta)$ describing the dependence of the radius of curvature of the profile on the angle of inclination β of the normal $\mathbf{n}$ to the profile.

We note that, if the profile configuration is given in the parametric form, $x = x_\Gamma(\alpha)$, $y = y_\Gamma(\alpha)$, with a parameter α being a monotonic function of the arc abscissa, the function $F(\beta)$ can always be determined, at least, numerically. For certain profiles this function can be determined in the analytical form. At the same time, the function $F(\beta)$ itself can be regarded as a means of preassigning the profile shape. In fact, the angle of inclination β of the normal $\mathbf{n}$ to the profile can well serve as a parameter of the equation of a smooth convex profile. In accordance with Fig. 1b and definition (4.5) of function $F(\beta)$ we obtain

$$\frac{dx_\Gamma}{d\beta} = \frac{dx_\Gamma}{ds}\frac{ds}{d\beta} = -F(\beta)\sin\beta, \qquad \frac{dy_\Gamma}{d\beta} = \frac{dy_\Gamma}{ds}\frac{ds}{d\beta} = F(\beta)\cos\beta.$$

As a result, the parametric equation of profile Γ can be written in the form:

$$\beta \in [0, \pi]:\ x_\Gamma(\beta) = 1 - \int_0^\beta F(\beta)\sin\beta\, d\beta, \qquad y_\Gamma(\beta) = \int_0^\beta F(\beta)\cos\beta\, d\beta. \tag{5.5}$$

We note that the choice of the angle of inclination β of the normal $\mathbf{n}$ to the profile as the parameter of the profile equations (5.5) ensures its convexity. At the same time, the profile closure and its correspondence to the given normalization are open to question. Because of this, it must be required that the function $F(\beta)$ be subject to two conditions

$$\int_0^\pi F(\beta)\cos\beta\, d\beta = 0, \qquad \int_0^\pi F(\beta)\sin\beta\, d\beta = 2, \tag{5.6}$$

where the former condition ensures the profile closure and the latter corresponds to the given normalization.

6. EXAMPLES AND DISCUSSION OF THE RESULTS

We will present the examples of determining the meniscus configuration for two particular fiber profiles, namely, an ovoid and an ellipse. We note that in calculating the Schwarz integral (4.14) the methods of discrete fast Fourier transformation (FFT) can be used. In the case, in which the function $F_*(\sigma)$ and, in essence, $F(\beta)$, is described by a finite number of harmonics, the problem solution is exact in the sense of the determination of the functions $\chi(\zeta)$ and $W(\zeta)$. At the same time, the economy of the FFT method, as concerned with computer resources, allows one to hope that the approximation will be fairly good even in the case of not too smooth functions $F(\beta)$. For the integration according to the Khristianovich formulas (5.4) the standard integration means of the MATLAB package can be used.

An ovoid as the fiber profile. We will take for $F(\beta)$ a function of the form:

$$F(\beta) = D_1 + D_2\cos\beta + D_3(1 + \cos\beta)^4[16 - (1 + \cos\beta)^4].$$

If the coefficients D_1, D_2, and D_3 are taken in the form:

$$D_1 = (R_D + R_B)/2, \qquad D_2 = (R_D - R_B)/2, \qquad D_3 = 4(R_B - R_D)/181,$$

where $R_D = F(0)$ and $R_B = F(\pi)$ are the radii of curvature of profile Γ at points D and B, then the profile closure condition, that is, the first condition (5.6), is absolutely fulfilled.

We will then take $R_D = 0.06$ and $R_D = 0.997296$. Then the normalization condition, that is, the second condition (5.6), is fulfilled accurate to 10^{-7}. As a result, the plot of the function $F(\beta)$ takes the form presented in Fig. 3a, while the fiber profile Γ reconstructed from Eq. (5.5) is shaped as an ovoid (Fig. 3b).

Setting, say, $\varepsilon = 0.1$ and using equations of Sections 4 and 5 we can reconstruct the configuration of the contact line Γ_c and the entire meniscus $\Sigma^{(u)}$ formed due to the capillary rise of the liquid along the fiber with the ovoidal profile presented in Fig. 3b in the case of the complete wetting of the fiber material by the liquid.

In Fig. 3c and 3d, we have plotted the projections of the contact line Γ_c on the planes x, z and y, z, respectively (the projection of this line on the x, y plane coincides with the fiber profile Γ). In the left lower corner of Fig. 3d an enlarged fragment of a vicinity of point D is presented; it illustrates the smooth nature of the contact line at this point. The fragment size is 0.003. The nodes on the contact line are the images of the division of interval $\sigma \in [0,\ 2\pi]$ into 2^{11} equal intervals for the discrete FFT.

Figure 4 presents the spatial view on the meniscus $\Sigma^{(u)}$; here, the black line corresponds to the contact line Γ_c, while the fiber itself is not presented.

From the results presented above it follows that a local increase in the fiber profile curvature leads to the local lowering in the liquid level on the fiber. This conclusion is confirmed by the results of investigations of other authors (see, for example, [11]).

Ellipse with the semiaxes a and b as the fiber profile. In accordance with the normalization, we take $a = 1$ and $b \in (0,\ 1]$. Obviously, the parametric equation of profile Γ can be preassigned using the parameter $\alpha \in [0,\ \pi]$

$$\Gamma:\ \ x_\Gamma(\alpha) = \cos\alpha, \qquad y_\Gamma(\alpha) = b\sin\alpha. \tag{6.1}$$

The angle of inclination β of the normal $\mathbf{n}$ to the ellipse can be related with the parameter α by means of the differential equation (see Fig. 1b)

$$\tan\left(\beta - \frac{\pi}{2}\right) = \frac{y'_\Gamma(\alpha)}{x'_\Gamma(\alpha)},$$

which, written in terms of Eq. (6.1), takes the form: $\tan\alpha = b\tan\beta$. Hence follows that

$$\alpha(\beta) = \arctan(b\tan\beta). \tag{6.2}$$

In accordance with definition (4.5), the function $F(\beta)$ can be found from the formula

$$\beta \in [0,\ \pi]:\ \ F(\beta) = \frac{d\alpha}{d\beta}\left[\left(\frac{dx_\Gamma}{d\alpha}\right)^2 + \left(\frac{dy_\Gamma}{d\alpha}\right)^2\right]^{1/2}\Bigg|_{\alpha=\alpha(\beta)}.$$

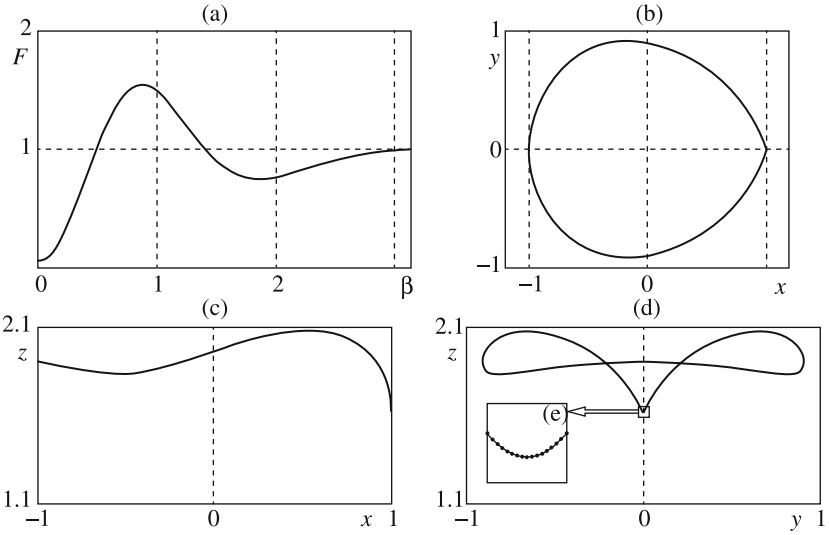

Fig. 3. Plot of the function $F(\beta)$ (a), fiber profile Γ (b), projections of the contact line Γ_c on the planes $x,\ z$ (c) and $y,\ z$ (d) for the fiber with an ovoidal profile, and enlarged fragment of the contact line in the vicinity of point D (e).

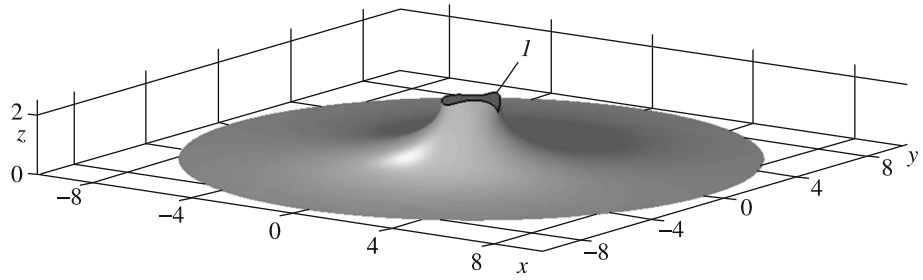

Fig. 4. View in space $x,\ y,\ z$ on the meniscus $\Sigma^{(u)}$ formed on the fiber with an ovoidal profile; (*1*) is the contact line Γ_c, the fiber itself is not presented.

In view of expressions (6.1) and (6.2), we obtain

$$\beta \in [0,\ \pi]: \quad F(\beta) = \frac{b}{\cos^2\beta\ +\ b^2\sin^2\beta}[\sin^2\alpha(\beta)\ +\ b^2\cos^2\alpha(\beta)]^{1/2}.$$

Using Eq. (6.2) the auxiliary relations can easily be derived

$$\sin^2\alpha\ +\ b^2\cos^2\alpha = \frac{b^2\cos^2\alpha}{\cos^2\beta}, \qquad \cos^2\beta\ +\ b^2\sin^2\beta = \frac{\cos^2\beta}{\cos^2\alpha}.$$

Using these relations we determine the final form of the function $F(\beta)$

$$\beta \in [0,\ 2\pi]: \ \ F(\beta) = b^2[\cos^2\beta\ +\ b^2\sin^2\beta]^{-3/2}.$$

Here, the domain of definition of the function is symmetrically continued onto the entire interval $\beta \in [0,\ 2\pi]$ with account for the profile symmetry about the x axis.

Given certain values of ε and b and using formulas of Sections 4 and 5 we can reconstruct the configurations of the contact line Γ_c and the entire meniscus $\Sigma^{(u)}$ formed due to the capillary rise of the liquid along the fiber with the elliptic profile in the case of complete wetting of the fiber material by the liquid.

Prior to choose a particular value $b \in [0,\ 1]$ we note that an interest in the elliptic profile is due, primarily, to two facts. An ellipse is a smooth profile, which ensures the smoothness of the generating meniscus Σ and the contact line Γ_c in the sense of the smoothness of the function $h(x,\ y)$ determining them. At the same time, in the maximum eccentricity limit, as $b \to 0$, the ellipse degenerates into a rectilinear segment, that is, a nonsmooth profile including two bend points; thus, an elliptic fiber transforms into a band-shaped one.

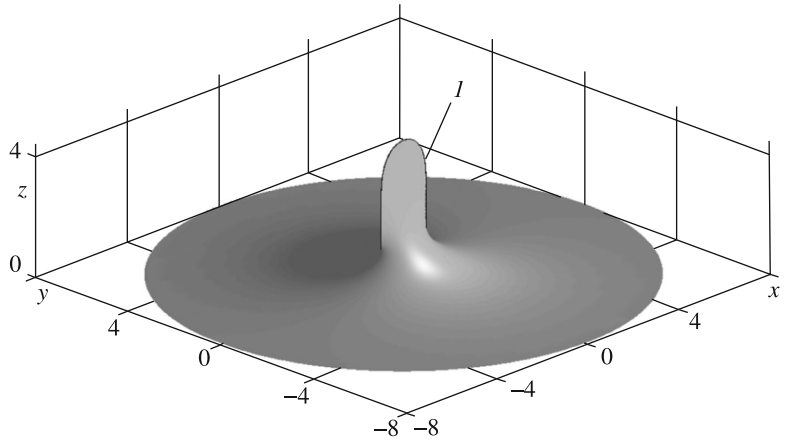

Fig. 5. General view of the meniscus $\Sigma^{(u)}$ for the fiber profile in the form of an ellipse with the semiaxes $a = 1$ and $b = 0.01$; $\gamma = 0$ and $\varepsilon = 0.1$; (*1*) is the contact line Γ_c, the fiber itself is not presented.

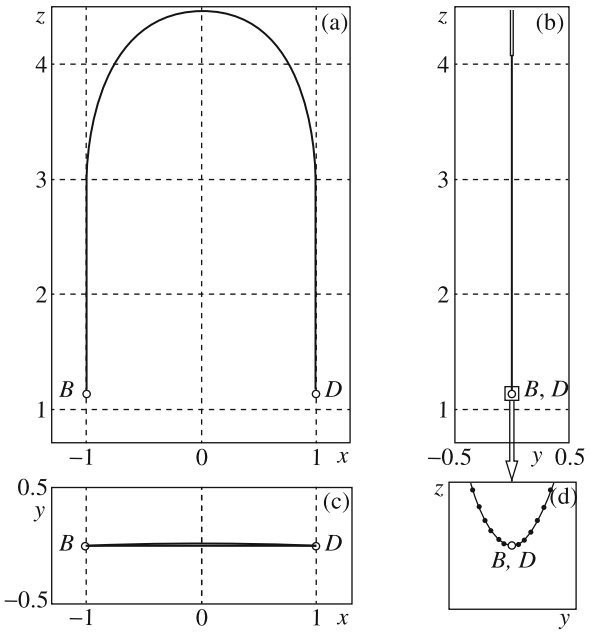

Fig. 6. Projections of the contact line Γ_c on the planes x, z (a), y, z (b), and x, y (c) for the fiber profile in the form of an ellipse with the semiaxes $a = 1$ and $b = 0.01$; $\gamma = 0$ and $\varepsilon = 0.1$; (d) is the enlarged fragment of the contact line in the vicinity of points B and D; the fragment size is of the order of 10^{-12}.

As shown in [24, 25], for this profile the solution of problem (1.1)–(1.5) with a smooth function $h(x, y)$ does not exist. Moreover, in the recent study [26] it was established that on the sharp edges of a band-shaped fiber the gradient $|\nabla h^{(u)}(x, y)|$ increases without bounds, while the function $h^{(u)}(x, y)$ itself undergoes jumps.

In view of an interest in the degenerated case the reconstruction of the complete form of the meniscus $\Sigma^{(u)}$ was performed for the elliptic fiber profile with the semiaxes $a = 1$ and $b = 0.01$ (Fig. 5). The Bond number was taken as $\varepsilon = 0.1$, The number of divisions of the interval $\sigma \in [0, 2\pi]$ in FFT was 2^{12}. In Fig. 6a, 6b, and 6c, we have plotted the projections of the contact line Γ_c of this meniscus on the planes (x, y), (x, z), and (y, z), respectively. To convince ourselves in the formally smooth nature of the contact line at points B and D we increased the number of divisions of the interval $\sigma \in [0, 2\pi]$ up to 2^{23} (see Fig. 6d, where an enlarged fragment of the contact line in the vicinity of points B and D is presented. The fragment size is of the order of 10^{-12}.

Near points B and D the contact line Γ_c includes certain regions, whose length is comparable with that of Γ_c itself and where the gradient $|\nabla h^{(u)}(x, y)|$ takes large values. This seems to be an important argument in favor of the adequacy of the conclusions made in [26] (obviously that any rigorous proofs of these

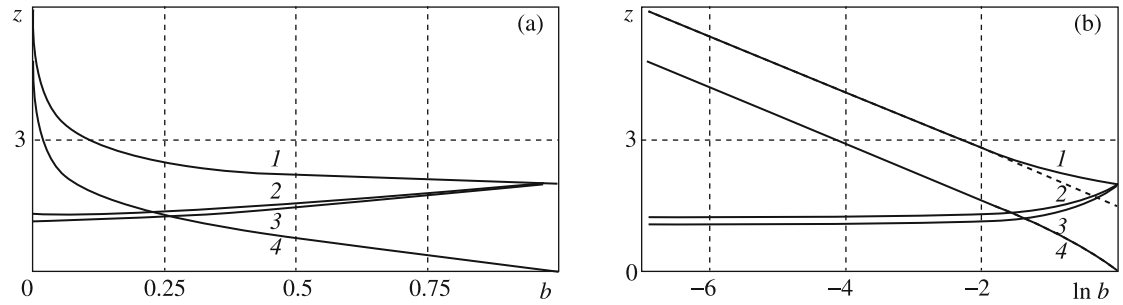

Fig. 7. Quantities h_C (*1*), h_B (*3*), and $\Delta h_{BC} = h_C - h_B$ (*4*) as functions of b (a) and $\ln b$ (b); $\gamma = 0$ and $\varepsilon = 0.1$; (*2*) is the height of the contact line on a round fiber with the same perimeter as that of the elliptic fiber for the same values of γ and ε [12]; the broken line is estimate (6.3) of the asymptotic dependence $h_C(b)$, as $b \to 0$.

conclusions cannot be obtained within the framework of the solution of the problem for an elliptic fiber).

At the same time, the large difference between the maximum h_C and minimum h_B liquid levels at the points of the contact line Γ_c for $b = 0.01$ poses a question of how these levels depend on the value of b. For this reason, we performed a set of calculations for different $b \in (0,\ 1]$. The minimum calculated value of the minor semiaxis was $b = 0.001$; in this case, the number of the divisions of the interval $\sigma \in [0,\ 2\pi]$ in the FTT was 2^{14}.

In Fig. 7a we have plotted the dependences of the liquid level h_C at point C (curve *1*), the liquid level h_B at point B (curve *3*), and the difference between these levels $\Delta h_{BC} = h_C - h_B$ (curve *4*) on the ellipse semiaxis b. For the sake of comparison, the contact line height on a round fiber [12] of the same perimeter as that of the elliptic fiber is also presented for the same values $\gamma = 0$ and $\varepsilon = 0.1$ is presented (curve *2*). Obviously, the $h_C(b)$ dependence is somewhat unclear in the vicinity of small b. To elucidate its nature in Fig. 7b we have presented the dependences of the same quantities, as in Fig. 7a, but on the quantity $\ln b$.

An analysis of the data obtained leads to the following estimates of the asymptotic dependences $h_B(b)$ and $h_C(b)$, as $b \to 0$, for $\varepsilon = 0.1$ (cf. Fig. 7b)

$$\varepsilon = 0.1, \quad b \to 0: \quad h_B(b) \approx 1.1306, \qquad h_C(b) \approx -\frac{2}{\pi}\ln b + 1.5365, \tag{6.3}$$

that is, the liquid level h_C at point C increases without bounds, as $b \to 0$. This physically unreal behavior of the solution of the problem of the inner asymptotic expansion (the fiber vicinity is the zone of the inner expansion) calls for explanations.

In [12] the formulation of the inner asymptotic expansion problem (1.5). (1.7)–(1.10) and the entire pattern of the asymptotic analysis of the problem of the capillary rise of a liquid along a fiber at small ε were based on the natural assumption that the order of the function $h(x,\ y)$ is everywhere, including the fiber vicinity, $O(\varepsilon^0) = O(1)$. Estimate (6.3) contradicts this assumption. However, this does not indicate that the assumption itself is incorrect but only that the derivation of the boundary value problem (1.5), (1.7)–(1.10), as the problem of inner asymptotic expansion, becomes apparently incorrect under the conditions of small curvature of the fiber profile curvature Γ and a small value of the contact angle γ.

In fact, the main equation (1.7) in this formulation was obtained from the general capillarity equation (1.4) by discarding the right hand side of this equation as a quantity of the order $O(\varepsilon)$ compared with the two terms on the left side having the order $O(1)$. However, at small values of the contact angle γ in a very thin zone adjoining the fiber there occur very large values of the absolute value $|\nabla h(x,\ y)|$, which enters into the denominators of both terms on the left side of Eq. (1.4) and which, correspondingly, can considerably diminish these terms in the order and make them comparable with $O(\varepsilon)$. Therefore, in this narrow zone adjoining the fiber (actually, within one more boundary layer) it is necessary to take Eq. (1.4) in its completeness as the basic equation. At $\gamma = 0$ and in the presence of small-curvature regions on the fiber profile Γ neglecting this boundary layer leads to inadequate estimate (6.3) of the absolute level of the liquid in the vicinity of the fiber.

Summary. Within the framework of the asymptotic analysis proposed in [12] under the assumption on the complete wetting of the fiber material an analytical solution of the problem of determining the meniscus shape is derived for a thin fiber, whose profile belongs to the class of smooth and convex profiles. The particular examples of the meniscus configuration are presented in the cases in which the fiber profile takes the shape of an ovoid or an ellipse. It is shown that the behavior of the contact line is rather nontrivial. It is established that in the presence of small curvature regions on the fiber profile and at small values of the contact angle the pattern of the asymptotic analysis of problem [12] must include one more boundary layer adjoining the fiber, within which the complete capillarity equation (1.4) is fulfilled.

The study was carried out with the support of the Russian Foundation for Basic Research (project No. 15-01-06029) and the National Science Foundation (POL-S1305338 and IOS-1354956).

REFERENCES

1. A.W. Adamson and A.P. Gast, *Physical Chemistry of Surfaces*, Wiley, New York (1997).
2. D.A. White and J.A. Tallmadge, "Static Menisci on the Outside of Cylinders," J. Fluid Mech. **23**, 325 (1965).
3. M.J. Scick, *Surface Characteristics of Fibers and Textiles*, Marcel Dekker, New York (1977).
4. J.C. Maxwell, *Capillary Action*, Encyclopaedia Britannica (1875).
5. D.F. James, "The Meniscus on the Outside of a Small Circular Cylinder," J. Fluid Mech. **63**, 657 (1974).
6. D.W. Langbein, *Capillary Surfaces: Shape – Stability – Dynamics, in Particular under Weightlessness*, Springer, New York (2002).
7. L.L. Lo, "The Meniscus on a Needle – a Lesson in Matching," J. Fluid Mech. **132**, 65 (1973).
8. D. Quere and J.M. di Meglio, "The Meniscus on a Fiber," Adv. Colloid Interface Sci. **48**, 141 (1994).
9. S.Q. Zhu and D.E. Hirt, "Improving the Wettability of Deep-Groove Polypropylene Fibers by Photografting," Textile Res. J. **79**, 534 (2009).
10. C. Duprat, C. Protière, A.Y. Beebe, and H.A. Stone, "Wetting of Flexible Fibre Arrays," Nature **482**, 510 (2012).
11. C. Pozrikidis, "Computation of Three-Dimensional Hydrostatic Menisci," IMA J. Appl. Math. **75**, 418 (2010).
12. M.M. Alimov and K.G. Kornev, "Meniscus on a Shaped Fibre: Singularities and Hodograph Formulation," Proc. Roy. Soc. London Ser. A **470**, 20140113 (2014).
13. R.I. Nigmatullin, *Dynamics of Multiphase Media*, Hemisphere Publ. Corp., New York (1990).
14. A. Nayfeh, *Perturbation Methods*, Wiley, New York (1973).
15. R. Courant, *Dirichlet's Principle, Conformal Mapping, and Minimal Surfaces*, Interscience (1950).
16. M.G. Bernadiner and V.M. Entov, *Hydrodynamic Theory of Anomalous Fluid Flows in Porous Media* [in Russian], Nauka, Moscow (1975).
17. V.V. Sokolovskii, "Nonlinear Seepage Flows of Ground Waters," Prikl. Mat. Mekh. **13**, 525 (1949).
18. H. Lamb, *Hydrodynamics*, Cambridge Univ. Press, Cambridge (1932).
19. S.A. Khristianovich, "Motion of Underground Waters which Does not Obey the Darcy Law," Prikl. Mat. Mekh. **4**, 33 (1940).
20. S.A. Chaplygion, *Gas Jets* [in Russian], Gostekhizdat, Moscow & Leningrad (1949).
21. M.A. Lavrent'ev and B.V. Shabat, *Methods of Theory of Functions of a Complex Variable* [in Russian], Nauka, Moscow (1973).
22. M.I. Gurevich, *Theory of Jets in Ideal Fluids*, Acad. Press, New York (1965).
23. F.D. Gakhov, *Boundary Value Problems* [in Russian], Fizmatgiz, Moscow (1963).
24. J.R. King, J.R. Ockendon, and H. Ockendon, "The Laplace–Young Equation near a Corner," Quart. J. Mech. Appl. Math. **52**, 73 (1999).
25. M.M. Alimov and K.G. Kornev, "Singularities of Meniscus at the V-Shaped Edge," Mech. Re. Commun. **62**, 162 (2014).
26. M.M. Alimov and K.G. Kornev, "Piercing the Water Surface with a Blade: Singularities of the Contact Line," Phys. Fluids **28**, 012102 (2016).